ACS EARTH AND SPACE CHEMISTRY

Open Access

http://pubs.acs.org/journal/aesccq

Article

Can Boronyl-Bearing Carbon Chains Serve as Gas-Phase Molecular Carriers of Interstellar Boron?

Cinthya K. Prieto-García, Heidy M. Quitián-Lara, Josep M. Masqué, Felipe Fantuzzi,* and J. Oscar C. Jiménez-Halla*

Cite This: *ACS Earth Space Chem.* 2025, 9, 2045−2055

Read Online

ACCESS | Metrics & More | Article Recommendations | Supporting Information

ABSTRACT: Boron is an exotic element in space. However, although no boron-bearing molecules have yet been identified in the interstellar medium (ISM), its unique chemical properties suggest that it could play a pivotal role in astrobiology and the origins of life. Given the isoelectronic relationship between the cyano (CN) and boronyl (BO) groups and the widespread detection of HC_nCN carbon chains in the ISM, we herein computationally investigate the potential of analogous BO-bearing chains (HC_nBO, n = 1−12) as viable gas-phase carriers of interstellar boron. Our calculations indicate that HC_nBO species exhibit lower enthalpies of formation and higher dipole moments than their CN-bearing counterparts, suggesting enhanced intrinsic stability and potential for detection via rotational spectroscopy. However, analysis of their formation and destruction pathways reveals that BO-bearing chains are susceptible to exergonic decomposition through reactions with CN radicals and H^- anions, which may significantly affect their abundances in the ISM. These findings underscore that, while HC_nBO systems emerge as theoretically attractive interstellar boron carriers, competitive decomposition and the element's low cosmic abundance pose substantial challenges to their astrophysical detection.

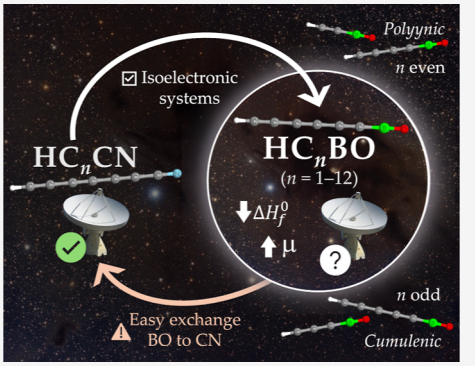

KEYWORDS: *astrochemistry, DFT calculations, boronyl group, cyanopolyynes, interstellar medium, dipole moment, rotational spectroscopy, formation and destruction pathways*

INTRODUCTION

Boron is a metalloid element in Group 13 of the periodic table, and its chemical behavior is largely governed by its electron deficiency. With only three valence electrons, boron typically adopts electron-deficient, trigonal-planar bonding modes (e.g., BR_3) and readily accommodates an additional lone pair through coordination, forming tetrahedral borate units.[1,2] Its chemistry is further enriched by its ability to form B−B single, double, and triple bonds,[3] enabling the construction of extended boron frameworks and unique polyhedral structures such as boranes and carboranes.[4,5] This remarkable versatility underpins its reactivity and has led to its use in diverse fields, including pharmaceuticals,[6] boron neutron capture therapy for cancer treatment,[7] nuclear radiation shielding,[8] optoelectronic devices,[9−11] electroanalytical technologies,[12] and as a reagent for dinitrogen fixation and reduction.[13−15] Additionally, boron shares an isodiagonal relationship with silicon,[16] resulting in intriguing chemical parallels in electronegativity, bonding, and reactivity.[17,18] These factors collectively highlight the unique position of boron in both fundamental and applied chemistry.

From a cosmochemical perspective, boron occupies a distinctive place among the light elements. Unlike carbon, nitrogen, or oxygen, it is not synthesized in stellar interiors at high temperatures (~5×10^6 K) where it is rapidly destroyed. Instead, its nucleosynthesis is primarily attributed to galactic cosmic-ray spallation of C, N, and O nuclei, with additional contributions from neutrino-induced processes in supernovae that help explain the enhanced abundance of ^{11}B.[19−22] This spallative origin makes boron one of the rarer cosmic elements, and its abundance in the interstellar medium (ISM) is correspondingly low. For instance, the abundance of boron in the present-day solar photosphere is estimated as log ϵ(B) = 2.70 ± 0.20,[23] which corresponds to to a B/H number ratio of approximately 5×10^{-10}. Observations of diffuse clouds report similar gas-phase B/H ratios on the order of 10^{-10}.[21,24]

Despite its relatively low cosmic abundance, boron has long been recognized as a crucial player in prebiotic chemistry, particularly in the context of the RNA world hypothesis for the origin of life.[25−28] Experimental studies show that boric acid [$B(OH)_3$] and various borate minerals (e.g., ulexite, kernite, colemanite) form esters with 1,2-diol functionalities in carbohydrates, stabilizing pentoses such as ribose under alkaline conditions.[25,26] These esters slow ribose decomposition

Received: March 22, 2025
Revised: July 3, 2025
Accepted: July 7, 2025
Published: July 15, 2025

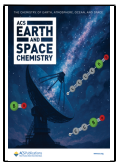

("browning") and have been proposed as a mechanism by which ribose could persist in prebiotic environments.[27,28] Indeed, borate's capacity to maintain ribose in its furanose form and facilitate the formation of pentose-borate esters offers a plausible pathway for the emergence of stable RNA precursors on early Earth.[25,26,29] Furthermore, boron-assisted reactions may extend beyond carbohydrate stabilization. Studies suggest that formamide-borate systems can simultaneously produce nucleic acid precursors and amino acid derivatives,[30,31] while recent findings indicate that boron also promotes polypeptide formation from amino acids under acidic and near-neutral conditions.[32] Collectively, these findings reinforce the idea that boron may have influenced multiple aspects of (bio)chemical evolution.

Beyond experimental evidence, boron has been detected in meteoritic samples and planetary materials. For example, olivine grains from the Itokawa asteroid exhibit homogeneous boron abundances of approximately 400 ppb.[33] On Mars, boron was identified in Gale Crater, where borate anions may either substitute for sulfate in calcium-sulfate veins or exist as a distinct phase that coprecipitated with calcium-sulfate as calcium-borates, with abundances below 0.05 wt % B.[34] These findings demonstrate that boron-bearing minerals can be incorporated into solid bodies within the solar system. However, whether similar minerals were sufficiently abundant on early Earth to stabilize ribose—and potentially polypeptides—remains debated, given the lack of geological records of borates older than 3.8 Ga.[35,36] Nonetheless, hypotheses involving tectonic recycling, weathering of boron-enriched crust, or evaporitic concentration provide plausible mechanisms for delivering borate to prebiotic environments.[29,37] Thus, while boron's prebiotic potential is well-documented experimentally, its cosmic history—encompassing high-energy production sites, transport through the interstellar medium, and eventual incorporation into planet-forming regions—remains an open question in astrochemistry and astrobiology.

A key unresolved issue is the absence of any confirmed boron-bearing molecules among the more than 330 species detected in interstellar and circumstellar environments.[38−40] While some boron may be sequestered in dust grains[24]—particularly given its oxophilic nature and its ability to replace silicon in silicate lattices—there may also be gas-phase carriers that have thus far eluded detection. In terrestrial laboratories, boron readily forms strong BO multiple bonds. The boronyl radical (BO) is isoelectronic with the cyano (CN) and ethynyl (CCH) radicals, both of which are prevalent in the ISM.[41] Moreover, numerous detected interstellar molecules contain the CN group, including linear cyano-bearing carbon chains (e.g., HC_nN)[42−48] and, more recently, aromatic and heterocyclic nitriles.[49−52] By analogy, BO and its carbon chain derivatives (HC_nBO) could represent viable interstellar species, particularly since laboratory studies show that BO reacts with unsaturated hydrocarbons to form stable boronyl compounds through exothermic, barrierless pathways.[41,53]

Given the many gaps in our understanding of boron's astrochemical origin, its potential role as a prebiotic reagent, and the established reactivity of boronyl compounds, this work investigates whether gas-phase boronyl chains might serve as carriers of interstellar boron. Specifically, we employ quantum chemical calculations to (i) evaluate the relative energies of candidate HC_nBO species, (ii) calculate chemical reactivity indices, (iii) predict key spectroscopic parameters (e.g., dipole moments), relevant to radioastronomical detection, (iv) ensure that candidate structures correspond to global minima, and (v) examine the thermochemical viability of their formation and destruction pathways. These data serve as essential prerequisites for guiding and interpreting future observational searches for boron-bearing molecules in the ISM.

COMPUTATIONAL DETAILS

All quantum-chemical calculations were performed using the Gaussian 09 package.[54] First, the geometries were optimized at the CAM-B3LYP-D3/def2-SVP level,[55−57] ensuring that all stationary points correspond to minima by verifying that all vibrational frequencies are real. We selected CAM-B3LYP based on its successful application to structurally related systems. Specifically, (i) CAM-B3LYP has been shown to accurately reproduce bond length alternation (BLA) patterns in *trans*-polyacetylene and polyynes,[58,59] (ii) it has been employed in several theoretical studies of interstellar carbon chains, including C_n^-, C_nH, and C_nN species,[60−62] and (iii) more recently, it has proven effective in describing the BLA of the cyclo[18]carbon system (C_{18}).[63] To further validate our choice, we performed benchmark calculations comparing CAM-B3LYP to the double hybrid functional B2PLYP,[64] as discussed in Section S1.1 of the Supporting Information, and found that CAM-B3LYP yields geometries and energetics in close agreement with B2PLYP, supporting its reliability for the systems studied.

To obtain more accurate thermochemical data, we reoptimized all structures using the G4 composite method,[65,66] which is widely recognized for its reliability in predicting properties such as enthalpies of formation, ionization energies, and electron affinities.[67] In addition, we evaluated the equilibrium rotational constants of the BO radical and the CN-bearing analogs, which exhibited consistently low relative deviations compared to reference values (see the Supporting Information for further details). These results collectively support the accuracy and consistency of our computational approach.[68,69]

Following G4 optimization, we calculated the adiabatic singlet−triplet energy gap (Δ_{ST}^{ad}), which is defined as the energy difference between the lowest singlet and triplet states at their corresponding optimized geometries. We also calculated the adiabatic ionization potential (IP^{ad}) and the electron affinity (EA^{ad}). For instance, Δ_{ST}^{ad} was evaluated as follows

$$\Delta_{ST}^{ad} = [\mathcal{E}_0(\mathbf{R}_T) + \mathcal{E}_{ZPE}(\mathbf{R}_T)] - [\mathcal{E}_0(\mathbf{R}_S) + \mathcal{E}_{ZPE}(\mathbf{R}_S)] \quad (1)$$

where $\mathcal{E}_{ZPE}$ stands for the zero-point vibrational energy, $\mathcal{E}_0$ is the electronic energy at 0 K, and $\mathbf{R}_T$ and $\mathbf{R}_S$ denote the equilibrium geometries of the triplet and singlet states, respectively.

The values of IP^{ad} and EA^{ad} were obtained similarly, with the energy difference between the cation or anion and the neutral state based on their respective optimized geometries. For simplicity, the main text presents only the values corresponding to the ground-state multiplicity of each neutral system. Additional results, such as vertical properties and chain growth until n = 20 using the CAM-B3LYP-D3/def2-SVP level, are provided in the Supporting Information. Furthermore, the bonding situation in optimized structures was elucidated via intrinsic bond orbital (IBO) analysis and is also shown in the Supporting Information.[70]

Dipole moments were extracted directly from the optimized geometries. In addition, enthalpies of formation (ΔH_f°) were

https://doi.org/10.1021/acsearthspacechem.5c00089
ACS Earth Space Chem. 2025, 9, 2045−2055

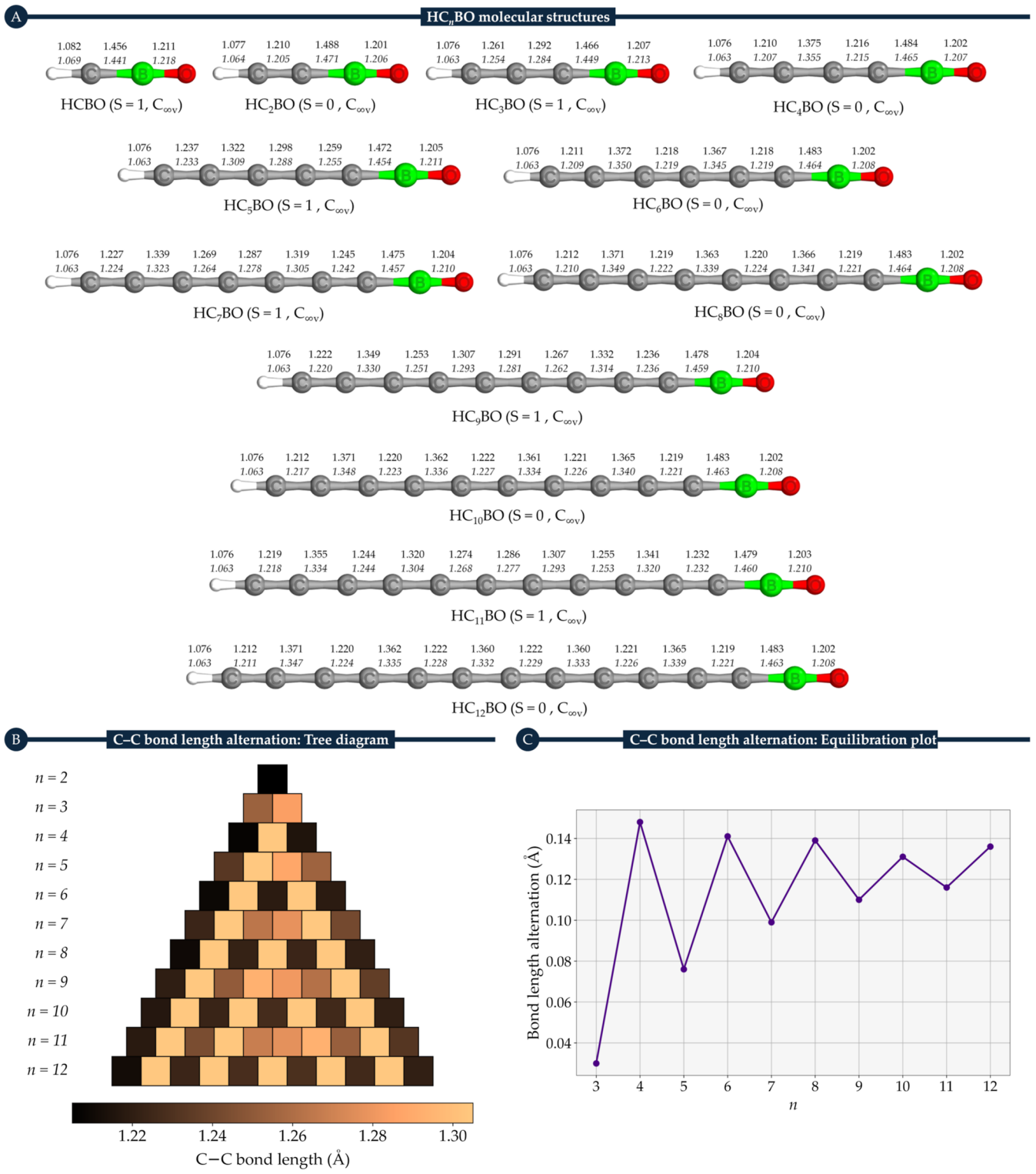

Figure 1. (A) Optimized ground-state geometries of the HC$_n$BO family (n = 1−12) obtained at the CAM-B3LYP-D3/def2-SVP and G4 levels (G4 results are shown in italics). Distances are reported in Å. (B) Tree diagram illustrating the variations in C−C bond lengths for HC$_n$BO systems (n = 2−12). (C) Plot of bond length alternation versus n, highlighting the bond length equilibration in smaller odd-numbered carbon chains (see text for details).

calculated from atomization energies, following the methodology described by Ochterski[71]

$$\sum D_0(M) = \sum_i n_i \mathcal{E}_0(X_i) - \mathcal{E}_0(\mathbf{R}_M) - \mathcal{E}_{\mathrm{ZPE}}(\mathbf{R}_M) \quad (2)$$

$$\Delta H_f^\circ(M, 0\mathrm{K}) = \sum_i n_i \Delta H_f^\circ(X_i) - \sum D_0(\mathbf{R}_M) \quad (3)$$

where $\sum D_0(M)$ is the total atomization energy of species M, and n_i is the number of atoms of type X_i. The standard enthalpies of

https://doi.org/10.1021/acsearthspacechem.5c00089
ACS Earth Space Chem. 2025, 9, 2045−2055

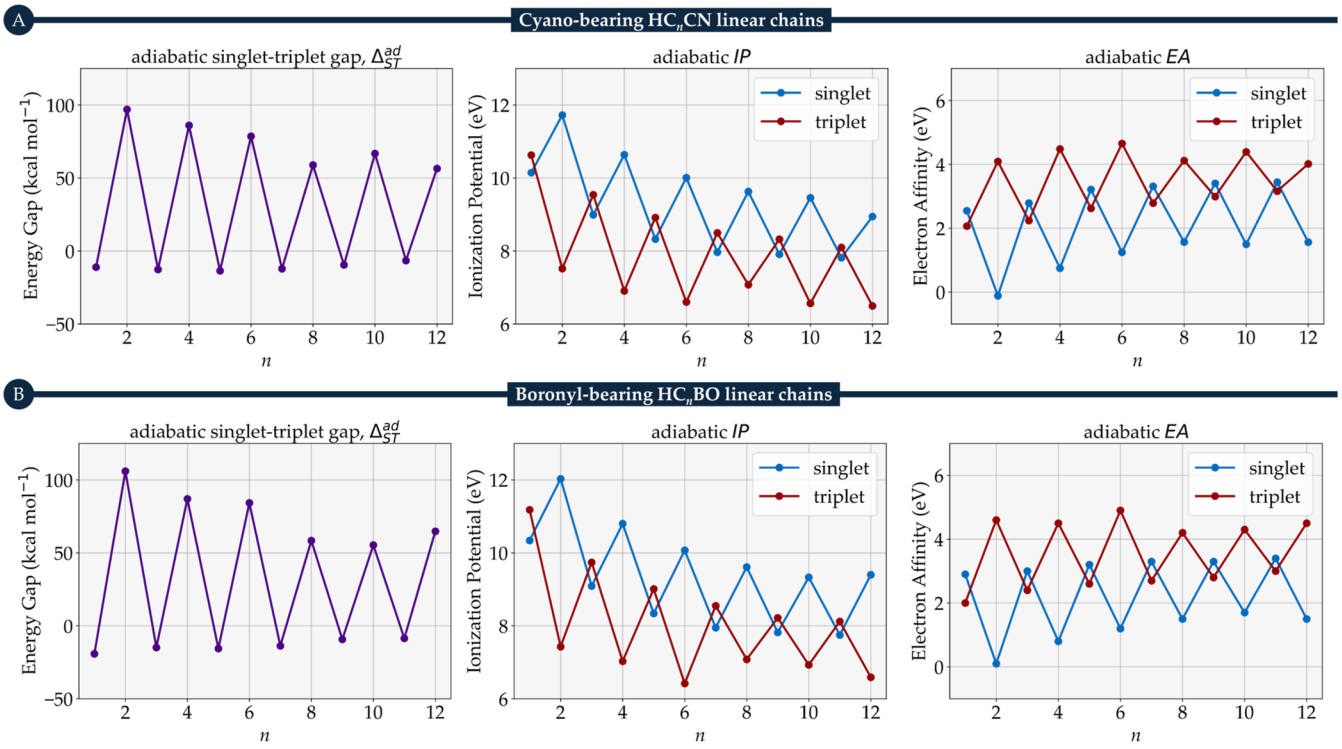

Figure 2. Comparison of adiabatic singlet−triplet gaps, ionization potentials, and electron affinities between the (A) HC$_n$CN and (B) HC$_n$BO families (n = 1−12) at the G4 level.

formation of the atomic elements were taken from the literature.[72]

For selected stoichiometries (n = 5, 6) in the HC$_n$BO series, we performed a comprehensive global minimum search using the AUTOMATON program.[73,74] Initial geometries were explored at the PBE/def2-SVP level and then reoptimized at CAM-B3LYP-D3/def2-SVP.[75] From these results, the lowest-energy isomers were further refined at the G4 level. In the case of HC$_6$BO linear isomers, we also performed analyses of natural bond orbital (NBO) and natural resonance theory (NRT) employing the NBO 7.0 program.[76,77] Furthermore, we analyzed the isomerization mechanism for HC$_6$BO to evaluate possible interconversions among its most stable forms. Energy barriers and transition states were confirmed through frequency calculations, ensuring that each transition state exhibited only one imaginary frequency.

To explore the reaction pathways leading to the formation of BO-bearing chains from known interstellar precursors, we calculated reaction energies, focusing on plausible formation and destruction channels. Single-point energy calculations were carried out at the CAM-B3LYP-D3/def2-TZVP level on geometries optimized at the CAM-B3LYP-D3/def2-SVP level,[56] to obtain more accurate relative energies for both the reaction channels and the isomerization mechanism.

RESULTS AND DISCUSSION

Structural Properties of HC$_n$BO Linear Chains. We begin by analyzing the structural properties of the HC$_n$BO family. As shown in Figure 1A, all lowest-energy (ground-state) structures of HC$_n$BO are essentially linear, featuring a B−O moiety at one terminus and a terminal hydrogen at the opposite end of the carbon chain. Notably, even-numbered chains (n = 2, 4, 6, ...) tend to adopt a *polyynic* bonding pattern, characterized by alternating triple and single C−C bonds, and favor a singlet closed-shell ground state. In contrast, odd-numbered chains (n = 1, 3, 5, ...) exhibit a *cumulenic* bonding arrangement, consisting of consecutive double bonds, and generally prefer a triplet open-shell ground state.

Although all systems remain linear at the CAM-B3LYP-D3/def2-SVP level, additional G4 optimizations revealed low-lying bent conformations for some even-numbered chains (notably n = 8 and n = 10). However, these bent geometries lie approximately 13 kcal mol^{-1} above their corresponding linear forms, reinforcing the preference for a linear arrangement featuring a B≡O bond as the global minimum. Indeed, IBO analyses (see Figure S2 in the Supporting Information) indicate a strong B−O triple bond, consistent with previous studies on boronyl-containing species.[41,53,78,79]

Boronyl chains exhibit a distinctive trend in C−C bond lengths. The terminal bonds measure approximately 1.22 Å (see Figure 1B), while those adjacent to the BO group are slightly longer. In even-numbered chains, the interior bonds alternate in length—successively measuring around 1.22 Å and 1.30 Å—reflecting their polyynic character. In contrast, odd-numbered chains lack this alternation, with central C−C bonds consistently ranging between 1.26 and 1.28 Å, indicative of a bond-length-equilibrated, cumulenic-like structure.

Analysis of C−C bond length alternation—which quantifies the range between the longest and shortest bonds in a chain (see Figure 1C)—provides further information about the bonding features. In this context, a near-zero variation signifies minimal differences in bond lengths, characteristic of an ideal cumulenic structure, whereas larger variations indicate pronounced bond length alternation. Even-numbered chains exhibit significant alternation, consistent with their polyynic arrangement. In contrast, odd-numbered chains generally show smaller variations. For n = 3, the bond length alternation is minimal, indicating a strong cumulenic character. As n increases, the

https://doi.org/10.1021/acsearthspacechem.5c00089
ACS Earth Space Chem. 2025, 9, 2045−2055

difference between odd- and even-numbered chains diminishes, suggesting that the bond length alternation in odd-numbered chains does not extend across the entire chain. Comparison with Figure 1B shows that larger odd-numbered chains indeed display cumulenic character predominantly in the interior, while their terminal regions exhibit an increasing polyynic character with increasing n.

These trends between even- and odd-numbered chains have been observed in several theoretical investigations of interstellar carbon chains, including the C_n^-, C_nH and C_nN families.[60−62] Moreover, CN-bearing carbon chains, which are analogs to boronyl carbon chains, have been reported to exhibit similar behavior in previous theoretical studies. For example, odd-numbered carbon chains (cyanopolyyne chains, $HC_{2n+1}N$ with n = 1−5) exhibit alternative triple and single C−C bonds, while even-numbered carbon chains (allenic chains, $HC_{2n}N$) have a cumulenic character.[68,69,80]

Chemical Reactivity Indices of Boronyl Chains. We now shift our focus to the chemical reactivity indices of boronyl chains, particularly their adiabatic singlet−triplet gaps, ionization potentials, and electron affinities. Figure 2 illustrates how these values vary with chain length n for the global minima, and also provides a comparison with the cyano-bearing analogues, HC_nCN. As previously discussed, even-numbered boronyl chains exhibit a closed-shell singlet ground state, as evidenced by positive adiabatic singlet−triplet gaps that place the triplet state at higher energy (see Figure 2, left panels). In contrast, odd-numbered chains display an open-shell triplet ground state, with negative adiabatic singlet−triplet gaps indicating that the singlet state is energetically higher. This behavior mirrors that of CN-bearing chains, where cyanopolyynes tend to favor a singlet ground state, while allenic chains exhibit a triplet ground state.[68,80]

Adiabatic singlet−triplet energy differences are generally larger in boronyl chains than in their cyano-bearing counterparts. Within both families, even-numbered chains exhibit greater absolute energy separations than odd-numbered chains, suggesting enhanced thermodynamic stability for the former. As the chain length increases, these energy gaps decrease, with odd-numbered chains approaching zero and even-numbered chains stabilizing at approximately 50 kcal mol^{-1}. This convergent behavior was further confirmed by analyzing boronyl chains up to n = 20 at the CAM-B3LYP-D3/def2-SVP level of theory, which continued to follow the observed trend, albeit at slightly different energy plateaus (see Figure S5 in the Supporting Information).

Local chemical descriptors, such as ionization potential and electron affinity, also shed light on the thermodynamic stability differences between singlet and triplet species. In both BO- and CN-bearing chains, even-numbered species with singlet ground states exhibit higher ionization potentials (see Figure 2, central panels), reflecting a greater difficulty in removing an electron compared to their triplet counterparts. Conversely, in odd-numbered chains, the triplet species display higher ionization potentials. Notably, the disparity between the ionization potentials of singlet and triplet states is more pronounced in even-numbered chains than in odd-numbered ones.

Regarding the adiabatic electron affinity values, an opposite trend emerges (see Figure 2, right panels). Even-numbered singlet chains exhibit the lowest electron affinities, suggesting that these neutral species are less prone to reduction, whereas their higher-energy triplet states show the greatest tendency to attract electrons and form anionic species. In contrast, odd-numbered chains display similar electron affinity values for both their ground-state triplet and their higher-energy singlet states, with the triplet states having slightly lower values. Overall, these results support the conclusion that even-numbered chains are thermodynamically more stable for both CN- and BO-bearing carbon chains.

From the comparative analysis between BO- and CN-bearing linear carbon chains, it is clear that both families exhibit similar behavior, as evidenced by the chemical reactivity indices in Figure 2. These indices consistently follow the same trends as the number of carbon atoms in the chain increases (see Figure S5 in the Supporting Information), and the vertical properties further support the stability of the singlet and triplet ground states (see Table S3 in the Supporting Information).

Chemical reactivity indices play a pivotal role in the development of astrochemical models and in identifying promising interstellar candidates. Owing to the high accuracy of the G4 composite computational method in calculating these properties,[65,67] the chemical data obtained in this study provide a reliable foundation to simulate the chemical evolution of both CN- and BO-bearing carbon chains in astronomical environments.

Dipole Moments and Enthalpies of Formation. Next, we turn our attention to the enthalpies of formation and dipole moments of the HC_nBO species. For all chain lengths, we compare these properties with those of the corresponding HC_nCN systems. Figure 3 displays a plot of these quantities for

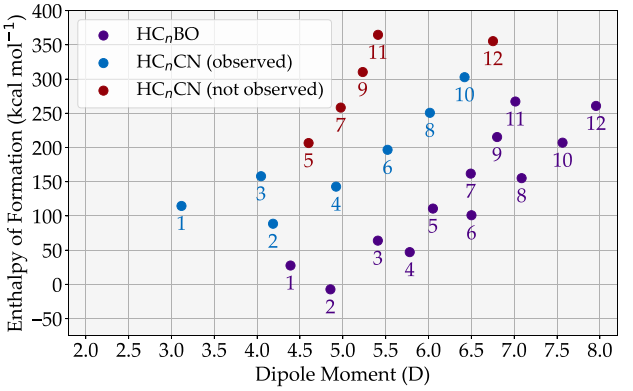

Figure 3. Dipole moments and enthalpies of formation of the HC_nBO and HC_nCN families (n = 1−12) at the G4 level.

both HC_nCN and HC_nBO species, covering n = 1−12. The figure also distinguishes between HC_nCN molecules that have been observed in the ISM and those that have not yet been detected.

The enthalpy of formation is a fundamental parameter for assessing the thermodynamic stability of chemical species, as it provides a direct energetic comparison between different compounds—with the compound exhibiting the lower enthalpy of formation deemed more stable.[69] In our analysis, we find that boronyl-bearing chains exhibit significantly lower enthalpies of formation than their CN-bearing analogs, indicative of enhanced thermodynamic stability. Across all chain lengths n, the enthalpy differences between isoelectronic boronyl and CN-bearing species exceed approximately 50 kcal mol^{-1}. Notably, the enthalpy of formation values of all BO-bearing compounds up to n = 12 are lower than that of $HC_{10}CN$, the longest carbon chain detected in astronomical environments. Overall, these results point toward a potential thermodynamic viability of BO-bearing

https://doi.org/10.1021/acsearthspacechem.5c00089
ACS Earth Space Chem. 2025, 9, 2045−2055

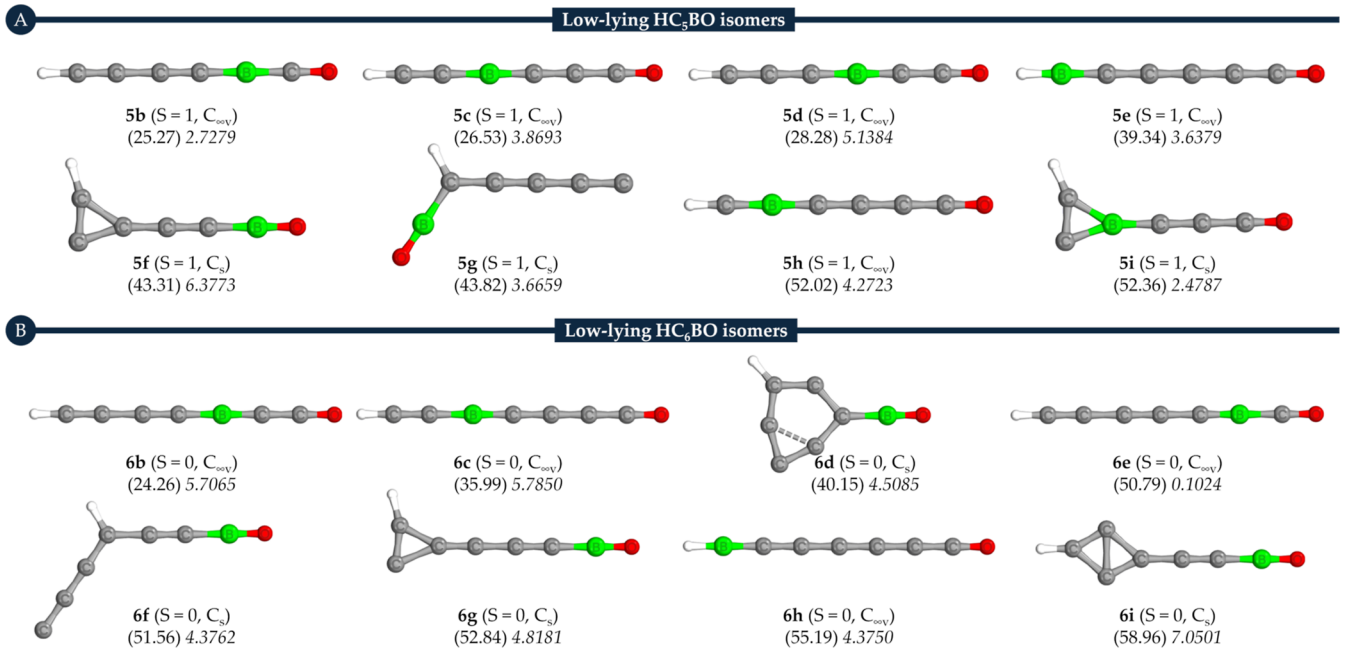

Figure 4. Optimized geometries of the most stable isomers with HC_nBO stoichiometry for (A) $n = 5$ and (B) $n = 6$ computed at the G4 level. Relative energies (kcal mol^{-1}) are indicated in parentheses, and dipole moments (Debye) are shown in italic.

species in the ISM, although any conclusive analysis must also consider additional factors such as decomposition pathways via chemical reactions and the influence of environmental conditions.

Molecular abundance is a critical factor for detectability in the ISM; however, the dipole moment is equally important, as the intensity of rotational transitions scales with the square of the dipole moment.[81−83] Notably, BO-bearing species exhibit higher dipole moments than their CN-bearing analogs, which suggests that they may be more amenable to astrophysical detection, provided that their abundances are sufficient (see Figure 3). Among the boronyl chains, HC_2BO emerges as the most promising candidate for detection across the series. It not only has the lowest enthalpy of formation—indicative of enhanced thermodynamic stability—but also features a significant dipole moment of 4.8554 D, making it a stronger target for identification via rotational spectroscopy.

The continuous integration of experimental, observational, and theoretical spectroscopic data, particularly rotational constants, is essential for the identification of new molecular species in the ISM. However, theoretical calculations of rotational constants are computationally demanding, and no experimental spectroscopic data currently exist for BO-bearing carbon chains. Fortunately, Tanimoto and colleagues recorded the microwave spectra of two isotopic variants, ^{11}BO and ^{10}BO, in the ground electronic state $X^2\Sigma^+$, reporting a rotational constant of 53165.5156 MHz.[84] These measurements were later compared against earlier experimental values of 53159.3 and 53149.0 MHz, respectively.[85] Our calculated equilibrium rotational constants for the BO radical are provided in the Supporting Information as part of a benchmarking analysis, which shows that the G4 method and CCSD(T) with large basis sets (e.g., aug-cc-pVQZ) reproduce the experimental value within 1% error, supporting the reliability of our computational approach.

Finally, some trends in the enthalpies of formation and dipole moments emerge across the series of carbon chains, warranting further discussion. One notable example is obtained when comparing the HC_nCN and HC_nBO systems as a function of n. By comparing an odd n entry with its subsequent even $n + 1$ counterpart, we find that the $n + 1$ species exhibit lower enthalpies of formation, reflecting enhanced thermodynamic stability. Additionally, these $n + 1$ species typically have larger dipole moments, as expected with increasing chain length.

Additionally, a convergent behavior emerges in the dipole moments of the $n + 2$ series for odd n values, suggesting that as the chain length increases the dipole moment tends toward a limiting value. In contrast, the dipole moments of the even n series show a more linear dependence on n. These observations underscore the complex interplay between chain length, molecular structure, and electronic properties in determining the stability and detectability of these species.

Minimum Energy Landscape. After obtaining detailed information on the enthalpies of formation and dipole moments of BO-bearing linear carbon chains, we now turn our attention to their relative stabilities compared to other potential isomers. This exploration is especially pertinent given that, for some stoichiometric formulas, distinct isomeric structures have been observed in the ISM. A notable example is acetic acid,[86] methyl formate,[87,88] glycolaldehyde,[89] and more recently 1,2-ethenediol[90]—all of which are $C_2H_4O_2$ isomers. Moreover, while the minimum energy principle suggests that the lowest-energy isomer should predominate in the ISM,[91] exceptions to this rule are well documented (e.g., $C_2H_4O_2$ isomers in Sgr B2(N)[92] and in the solar-type protostar NGC 1333 IRAS 4A[93]), since observed abundances depend not only on intrinsic stability but also on factors such as the efficiency of formation pathways[94] and preferential adsorption onto icy grain mantles.[95] Additionally, the charge state can significantly influence the energy ordering and structural features of these species, whether they are complex organic molecules[96,97] or polycyclic aromatic hydrocarbons.[98,99] Therefore, identifying low-lying isomers is crucial for pinpointing promising candidates for future observational detection.

https://doi.org/10.1021/acsearthspacechem.5c00089
ACS Earth Space Chem. 2025, 9, 2045−2055

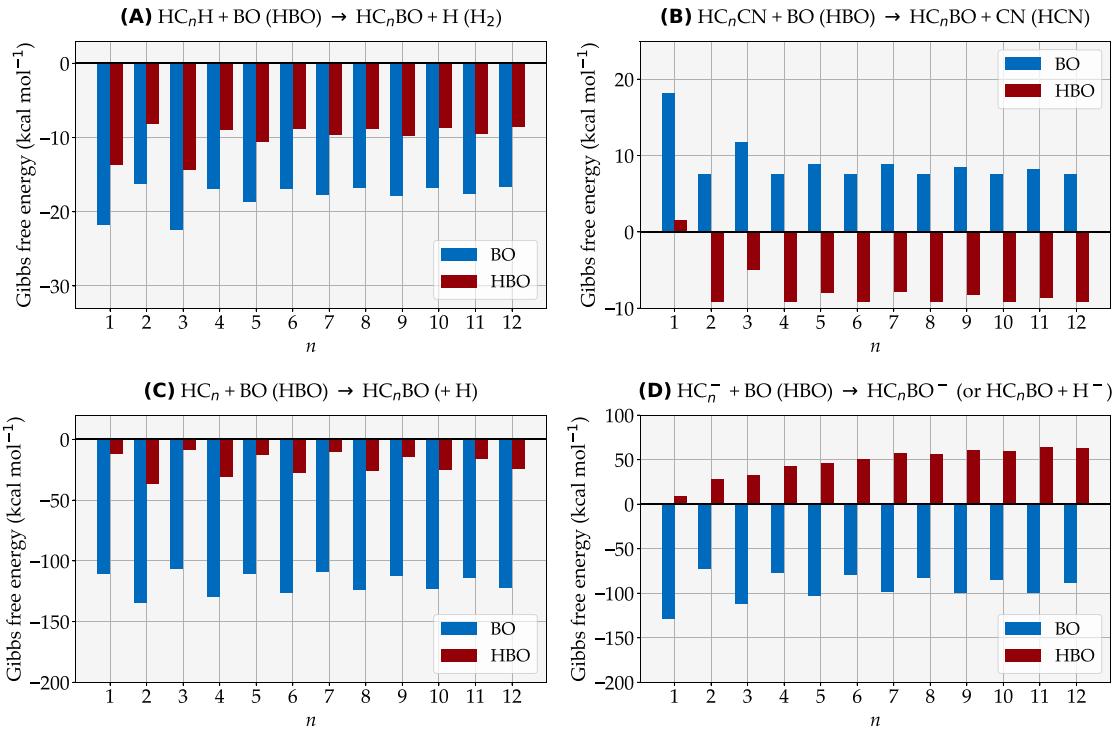

Figure 5. Formation (negative values) and destruction (positive values) channels of the boronyl chains (HC$_n$BO with n = 1−12). All Gibbs free energies are given in kcal mol^{-1}.

Here, we focus on exploring the potential energy surfaces (PES) for HC$_5$BO and HC$_6$BO, with the low-lying energy minima illustrated in Figure 4. Our analysis reveals that, for both stoichiometries, the two most stable isomers are linear structures featuring the oxygen and hydrogen atoms at opposite ends of the chain, with the only difference being the position of the boron atom. In both cases, the global minimum (GM) corresponds to the expected linear isomer in which the boron atom is directly bonded to the oxygen, thereby forming a stable BO group. This linear preference contrasts with that observed in other heteroatomic carbon chains, such as MgC$_n$H, whose global minima are cyclic for odd values of n.[100,101]

For HC$_5$BO (Figure 4A), the GM exhibits a significant dipole moment of 6.0516 D. The next most stable isomers, designated as **5b** and **5c**, possess lower dipole moments (2.7279 and 3.8693 D, respectively) compared to the GM. Although most isomers display reduced dipole moments, the **5f** isomer stands out with a relatively high dipole moment, which could facilitate its detection via rotational spectroscopy. However, its thermodynamic stability is, naturally, inferior to that of the GM. In general, among linear isomers where only the boron position varies, those with an odd number of carbon atoms between the boron and oxygen atoms (e.g., **5b** and **5c**) are more stable than those with an even number, likely due to the formation of a triple C−C bond along the chain between the boron and hydrogen atoms. Additionally, nonlinear isomers such as **5f** and **5g** are more stable than **5i** due to the stabilizing effect of the BO group.

In the case of HC$_6$BO (Figure 4B), isomers **6b** and **6c** exhibit similar dipole moments (5.7065 and 5.7850 D, respectively) and rank as the next most stable relative to the GM, which itself has a higher dipole moment (6.5013 D). Notably, the **6i** isomer has a larger dipole moment than the GM but is substantially less stable, with a relative energy of 58.96 kcal mol^{-1}. Among the linear isomers of HC$_6$BO, those with an even number of carbon atoms between the boron and oxygen atoms (e.g., **6b** and **6c**) are more stable than those with an odd number (e.g., **6e**), a trend attributed to the polyynic character on the left side of the chain (see Figure S7 in the Supporting Information). The **6b** structure is particularly stable due to the short carbon chain between boron and oxygen, whereas the **6h** structure is less stable as the chain extends to six carbon atoms. All lower-energy nonlinear isomers (**6d**, **6f**, **6g**, and **6i**) feature the BO group, which contributes significantly to their stability.

The discovery of the cyclic **6d** isomer prompted further investigation into the potential cyclization of boronyl chains, leading to the exploration of three types of rings: (n + 2)-membered heterocycles, n-membered rings, and six-membered rings (see Table S2 in the Supporting Information). However, all cyclization pathways were found to be endergonic, reinforcing the conclusion that the global minima for HC$_n$BO stoichiometries corresponds to BO-bearing linear structures.

These findings highlight once more the thermodynamic viability of BO-bearing linear structures as candidates for astrophysical detection. However, as earlier mentioned, interstellar abundances depend not only on thermodynamic stability but also on the availability of the chemical elements and of viable formation pathways. For example, the isomerization reaction from the **6h** structure to the more stable **6c** structure was found to be highly unfavorable under low-temperature conditions typical of dark molecular clouds (e.g., 10 K), due to a significant energy barrier of 66.21 kcal mol^{-1} despite being exergonic ($\Delta G^{\ddagger}_{reac}$ = −15.21 kcal mol^{-1}; see Figure S8 in the Supporting Information).

Formation and Destruction Channels. To explore the formation and destruction pathways of BO-bearing carbon chains of type HC$_n$BO (n = 1−12), we analyzed reactions involving boron-bearing reactants—specifically, the boronyl radical (BO) and boron hydride oxide (HBO)—with carbon chain families previously detected in astronomical environments

https://doi.org/10.1021/acsearthspacechem.5c00089
ACS Earth Space Chem. 2025, 9, 2045−2055

(HC_nH, HC_nCN, HC_n, and HC_n^-). The proposed reactions are summarized as follows

$$HC_nH + BO(HBO) \rightarrow HC_nBO + H(H_2) \quad (4)$$

$$HC_nCN + BO(HBO) \rightarrow HC_nBO + CN(HCN) \quad (5)$$

$$HC_n + BO(HBO) \rightarrow HC_nBO(+ H) \quad (6)$$

$$HC_n^- + BO(HBO) \rightarrow HC_nBO^-(\text{or } HC_nBO + H^-) \quad (7)$$

For the formation pathways starting from the carbon polyyne family (HC_nH), all reactions exhibit consistently exergonic behavior during chain growth for both BO and HBO reactants (see Figure 5A). A nearly constant energy difference of approximately 8 kcal mol^{-1} is observed between the two channels. Notably, the neutral−neutral reaction with the BO radical yields the most favorable (i.e., most negative) reaction energies. For chains with four or more carbon atoms, the reaction energies stabilize, remaining approximately constant at around −18 and −9 kcal mol^{-1}, respectively.

Experimental evidence supports these findings: HC_2BO and HC_4BO have been synthesized using crossed molecular beam techniques via reactions of the BO radical with acetylene (HC_2H) and diacetylene (HC_4H), yielding reaction energies of -14.82 ± 1.91 and -15.06 ± 2.63 kcal mol^{-1}, respectively.[53] Theoretical studies using CCSD(T)/cc-pVTZ and CCSD(T)/CBS methods reported formation energies of -13.86 ± 2.39 and -14.82 ± 2.39 kcal mol^{-1}, closely matching the experimental results.[102,103] Our own calculations yield values of −16.18 and −16.97 kcal mol^{-1}, further corroborating the thermodynamic feasibility of these processes.

In contrast, the formation of BO-bearing chains from cyano-bearing precursors via reaction with the BO radical is consistently endergonic, with reaction energies near ∼8 kcal mol^{-1} (see Figure 5B). This thermodynamic behavior implies that the reverse reaction—the destruction of BO-bearing chains through interaction with CN—is exergonic, thereby providing a feasible pathway for their decomposition. Given that CN is relatively abundant in dense interstellar clouds—with estimated equilibrium CN column densities on the order of 10^{13} cm^{-2} and CN/HCN density ratios often exceeding 10 in photon-dominated regions—this process could significantly limit the abundance of BO-bearing species in the ISM. Although kinetic barriers might inhibit this decomposition, the thermodynamic favorability suggests that such reaction could play an important role. Furthermore, when HBO is employed as the reactant, all pathways become exergonic—except for the case of $n = 1$, where the reaction (involving HCCN) requires approximately 1.48 kcal mol^{-1} to yield HCBO and HCN. For $n \geq 4$, the reaction energies remain nearly invariant with increasing chain length.

Figure 5C shows that formation pathways involving the HC_n family, when reacting with either boron-bearing species, are favorable and exergonic along the chain growth. In particular, reactions of the HC_nH family with the BO radical are especially favorable—coupling two radical species and yielding reaction energies as negative as −118 kcal mol^{-1}. In contrast, reactions involving the HC_n species are less exergonic, with an energy difference of about 98 kcal mol^{-1} between the BO and HBO channels, while remaining relatively constant across different chain lengths.

Figure 5D illustrates a destruction channel for boronyl chains in the presence of H^-, leading to the formation of HC_n^- species and HBO. The endergonicity of this reaction becomes more pronounced as the chain length increases, suggesting that interactions with H^- increasingly favor the breakdown of BO-bearing species in longer chains. H^- is a well-established astrophysical agent; it plays a pivotal role in providing bound-free opacity in cool stars (with photospheric temperatures below 7000 K) and is believed to have catalyzed molecular hydrogen formation in the early Universe—approximately 500,000 years after the Big Bang—thereby facilitating the cooling and collapse of gas clouds to form the first stars and protogalaxies.[104] Although its weak spectral signatures make direct detection in the diffuse ISM challenging, theoretical models consistently predict the presence of H^- at low abundances,[105] implying that it could indeed contribute to the destruction of BO-bearing carbon chains. In contrast, the formation of anionic boronyl chains is highly favorable, as indicated by Gibbs free energy values ranging between −72.88 and −128.77 kcal mol^{-1}.

CONCLUSIONS

In summary, our work investigates the potential of boronyl-bearing chains as gas-phase carriers of interstellar boron. Their stability was evaluated using enthalpy of formation, adiabatic singlet−triplet gaps, chemical reactivity indices, and potential energy surface analyses, while their intrinsic detectability potential was gauged through calculated dipole moments. Our results reveal that even-numbered boronyl chains, with their closed-shell singlet ground states and polyynic character, contrast with odd-numbered chains, which adopt open-shell triplet ground states with cumulenic character; these findings underscore their isoelectronic similarity to CN-bearing chains. Thermodynamically, BO-bearing chains consistently exhibit lower enthalpies of formation than their cyano analogs, a trend corroborated by chemical reactivity indices, and their larger dipole moments further support their potential for astrophysical detection. Detailed potential energy surface exploration of HC_5BO and HC_6BO stoichiometries confirms that the global minima correspond to linear BO-bearing structures, with alternative isomers lying significantly higher in energy and featuring high isomerization barriers and endergonic cyclization pathways, indicating that such linear forms are the most favored under the low-temperature conditions typical of dark molecular clouds. Although energetically favorable formation pathways—such as reactions of BO with HC_nH, HC_n, and HC_n^-—support the synthesis of these chains, our analysis also identifies viable destruction channels involving CN radicals and H^-, which, combined with the intrinsically low abundance of boron, pose significant challenges for their accumulation and detection in the ISM. Thus, while boronyl-bearing carbon chains present intriguing prospects as carriers of interstellar boron due to their favorable stability and spectroscopic properties, the balance between their formation and competitive decomposition reactions may ultimately render their detection extremely challenging, a factor that remains relevant given boron's potential role in astrobiology and the origins of life.

ASSOCIATED CONTENT

Supporting Information

The Supporting Information is available free of charge at https://pubs.acs.org/doi/10.1021/acsearthspacechem.5c00089.

Additional bonding and structural data; chemical properties, cyclization, and growth of BO-bearing carbon chains;

https://doi.org/10.1021/acsearthspacechem.5c00089
ACS Earth Space Chem. 2025, 9, 2045−2055

exploration of the potential energy surface of HC_nBO (n = 5−6); Cartesian coordinates (PDF)

AUTHOR INFORMATION

Corresponding Authors

Felipe Fantuzzi − *Chemistry and Forensic Science, School of Natural Sciences, University of Kent, Canterbury CT2 7NH, U.K.*; orcid.org/0000-0002-8200-8262; Email: f.fantuzzi@kent.ac.uk

J. Oscar C. Jiménez-Halla − *Departamento de Química, División de Ciencias Naturales y Exactas, Sede Noria Alta, Universidad de Guanajuato, Guanajuato 36050, Mexico*; Email: jjimenez@ugto.mx

Authors

Cinthya K. Prieto-García − *Departamento de Química, División de Ciencias Naturales y Exactas, Sede Noria Alta, Universidad de Guanajuato, Guanajuato 36050, Mexico*

Heidy M. Quitián-Lara − *Max Planck Institute for Extraterrestrial Physics, Garching 85748, Germany*

Josep M. Masqué − *Departamento de Astronomía, Universidad de Guanajuato, Guanajuato 36000, Mexico*

Complete contact information is available at: https://pubs.acs.org/10.1021/acsearthspacechem.5c00089

Notes

The authors declare no competing financial interest.

ACKNOWLEDGMENTS

J.O.C.J.H. acknowledges the facilities of the DCNyE, the Department of Chemistry, and the National Laboratory UG-CONAHCyT (LACAPFEM) of the University of Guanajuato. F.F. and H.M.Q.L. are grateful for financial support from the University of Kent and the Center for Astrochemical Studies at the Max Planck Institute for Extraterrestrial Physics (CAS@MPE). C.K.P.G. thanks CONAHCyT for a Ph.D. fellowship (1233185).

REFERENCES

(1) Schubert, D. M. Boron: Inorganic Chemistry. In *Encyclopedia of Inorganic and Bioinorganic Chemistry*; Wiley, 2019; pp 1−21.

(2) Petasis, N. A. Expanding Roles for Organoboron Compounds—Versatile and Valuable Molecules for Synthetic, Biological and Medicinal Chemistry. *Aust. J. Chem.* **2007**, *60*, 795.

(3) Braunschweig, H.; Dewhurst, R. D. Single, Double, Triple Bonds and Chains: The Formation of Electron-Precise B−B Bonds. *Angew. Chem., Int. Ed.* **2013**, *52*, 3574−3583.

(4) Lipscomb, W. N. The Boranes and Their Relatives. *Science* **1977**, *196*, 1047−1055.

(5) Grimes, R. N. *Carboranes*, 3rd ed.; Academic Press: London, 2016; p 1058.

(6) Grams, R. J.; Santos, W. L.; Scorei, I. R.; Abad-García, A.; Rosenblum, C. A.; Bita, A.; Cerecetto, H.; Viñas, C.; Soriano-Ursúa, M. A. The Rise of Boron-Containing Compounds: Advancements in Synthesis, Medicinal Chemistry, and Emerging Pharmacology. *Chem. Rev.* **2024**, *124*, 2441−2511.

(7) Dymova, M. A.; Taskaev, S. Y.; Richter, V. A.; Kuligina, E. V. Boron neutron capture therapy: Current status and future perspectives. *Cancer Commun.* **2020**, *40*, 406−421.

(8) Dong, M.; Zhou, S.; Xue, X.; Feng, X.; Sayyed, M.; Khandaker, M. U.; Bradley, D. The potential use of boron containing resources for protection against nuclear radiation. *Radiat. Phys. Chem.* **2021**, *188*, 109601.

(9) Ji, L.; Griesbeck, S.; Marder, T. B. Recent developments in and perspectives on three-coordinate boron materials: a bright future. *Chem. Sci.* **2017**, *8*, 846−863.

(10) Mellerup, S. K.; Wang, S. Boron-Doped Molecules for Optoelectronics. *Trends Chem.* **2019**, *1*, 77−89.

(11) Saalfrank, C.; Fantuzzi, F.; Kupfer, T.; Ritschel, B.; Hammond, K.; Krummenacher, I.; Bertermann, R.; Wirthensohn, R.; Finze, M.; Schmid, P.; Engel, V.; Engels, B.; Braunschweig, H. cAAC-Stabilized 9,10-diboraanthracenes—Acenes with Open-Shell Singlet Biradical Ground States. *Angew. Chem., Int. Ed.* **2020**, *59*, 19338−19343.

(12) Muzyka, K.; Sun, J.; Fereja, T. H.; Lan, Y.; Zhang, W.; Xu, G. Boron-doped diamond: current progress and challenges in view of electroanalytical applications. *Anal. Methods* **2019**, *11*, 397−414.

(13) Légaré, M.-A.; Bélanger-Chabot, G.; Dewhurst, R. D.; Welz, E.; Krummenacher, I.; Engels, B.; Braunschweig, H. Nitrogen fixation and reduction at boron. *Science* **2018**, *359*, 896−900.

(14) Légaré, M.-A.; Bélanger-Chabot, G.; Rang, M.; Dewhurst, R. D.; Krummenacher, I.; Bertermann, R.; Braunschweig, H. One-pot, room-temperature conversion of dinitrogen to ammonium chloride at a main-group element. *Nat. Chem.* **2020**, *12*, 1076−1080.

(15) Fantuzzi, F.; Moral, R.; Dewhurst, R. D.; Braunschweig, H.; Phukan, A. K. Probing the Potential of Hitherto Unexplored Base-Stabilized Borylenes in Dinitrogen Binding. *Chem. Eur. J.* **2022**, *28*, No. e202104123.

(16) Rayner-Canham, G. Isodiagonality in the periodic table. *Found. Chem.* **2011**, *13*, 121−129.

(17) Gilmer, J.; Bolte, M.; Virovets, A.; Lerner, H.; Fantuzzi, F.; Wagner, M. A Hydride-Substituted Homoleptic Silylborate: How Similar is it to its Diborane(6)-Dianion Isostere? *Chem. Eur. J.* **2023**, *29*, No. e202203119.

(18) Gilmer, J.; Trageser, T.; Čaić, L.; Virovets, A.; Bolte, M.; Lerner, H.-W.; Fantuzzi, F.; Wagner, M. Catalyst-free diboration and silaboration of alkenes and alkynes using bis(9-heterofluorenyl)s. *Chem. Sci.* **2023**, *14*, 4589−4596.

(19) Reeves, H.; Fowler, W. A.; Hoyle, F. Galactic Cosmic Ray Origin of Li, Be and B in Stars. *Nature* **1970**, *226*, 727−729.

(20) Woosley, S. E.; Hartmann, D. H.; Hoffman, R. D.; Haxton, W. C. The nu-process. *Astrophys. J.* **1990**, *356*, 272.

(21) Ritchey, A. M.; Federman, S. R.; Sheffer, Y.; Lambert, D. L. The abundance of boron in diffuse interstellar clouds. *Astrophys. J.* **2011**, *728*, 70.

(22) Liu, M.-C.; Chaussidon, M. The Cosmochemistry of Boron Isotopes. In *Advances in Isotope Geochemistry*, 2018; pp 273−289.

(23) Asplund, M.; Grevesse, N.; Sauval, A. J.; Scott, P. The Chemical Composition of the Sun. *Annu. Rev. Astron. Astrophys.* **2009**, *47*, 481−522.

(24) Howk, J. C.; Sembach, K. R.; Savage, B. D. The Abundance of Interstellar Boron. *Astrophys. J.* **2000**, *543*, 278−283.

(25) Ricardo, A.; Carrigan, M. A.; Olcott, A. N.; Benner, S. A. Borate Minerals Stabilize Ribose. *Science* **2004**, *303*, 196.

(26) Kim, H.-J.; Ricardo, A.; Illangkoon, H. I.; Kim, M. J.; Carrigan, M. A.; Frye, F.; Benner, S. A. Synthesis of Carbohydrates in Mineral-Guided Prebiotic Cycles. *J. Am. Chem. Soc.* **2011**, *133*, 9457−9468.

(27) Scorei, R. Is Boron a Prebiotic Element? A Mini-review of the Essentiality of Boron for the Appearance of Life on Earth. *Orig. Life Evol. Biosph.* **2012**, *42*, 3−17.

(28) Franco, A.; da Silva, J. A. L. Boron in Prebiological Evolution. *Angew. Chem., Int. Ed.* **2021**, *60*, 10458−10468.

(29) Grew, E. S.; Bada, J. L.; Hazen, R. M. Borate Minerals and Origin of the RNA World. *Orig. Life Evol. Biosph.* **2011**, *41*, 307−316.

(30) Saladino, R.; Barontini, M.; Cossetti, C.; Di Mauro, E.; Crestini, C. The Effects of Borate Minerals on the Synthesis of Nucleic Acid Bases, Amino Acids and Biogenic Carboxylic Acids from Formamide. *Orig. Life Evol. Biosph.* **2011**, *41*, 317−330.

(31) Franco, A.; Ascenso, J.; Ilharco, L.; Diogo, H.; André, V.; da Silva, J. Ribose-borate esters as potential components for prebiological evolution. *J. Mol. Struct.* **2019**, *1184*, 281−288.

(32) Sumie, Y.; Sato, K.; Kakegawa, T.; Furukawa, Y. Boron-assisted abiotic polypeptide synthesis. *Commun. Chem.* **2023**, *6*, 89−96.

(33) Fujiya, W.; Hoppe, P.; Ott, U. Boron abundances and isotopic ratios of olivine grains on Itokawa returned by the Hayabusa spacecraft. *Meteorit. Planet. Sci.* **2016**, *51*, 1721−1729.
(34) Gasda, P. J.; et al. In situ detection of boron by ChemCam on Mars. *Geophys. Res. Lett.* **2017**, *44*, 8739−8748.
(35) Grew, E. S.; Dymek, R. F.; De Hoog, J. C.; Harley, S. L.; Boak, J.; Hazen, R. M.; Yates, M. G. Boron isotopes in tourmaline from the ca. 3.7−3.8Ga Isua supracrustal belt, Greenland: Sources for boron in Eoarchean continental crust and seawater. *Geochim. Cosmochim. Acta* **2015**, *163*, 156−177.
(36) Franco, A.; Neves, M. O.; da Silva, J. A. Boron as a Hypothetical Participant in the Prebiological Enantiomeric Enrichment. *Astrobiology* **2023**, *23*, 605−615.
(37) Neveu, M.; Kim, H.-J.; Benner, S. A. The "Strong" RNA World Hypothesis: Fifty Years Old. *Astrobiology* **2013**, *13*, 391−403.
(38) Müller, H. S. P.; Thorwirth, S.; Roth, D. A.; Winnewisser, G. The Cologne Database for Molecular Spectroscopy, CDMS. *Astron. Astrophys.* **2001**, *370*, L49−L52.
(39) Müller, H. S.; Schlöder, F.; Stutzki, J.; Winnewisser, G. The Cologne Database for Molecular Spectroscopy, CDMS: a useful tool for astronomers and spectroscopists. *J. Mol. Struct.* **2005**, *742*, 215−227.
(40) The Cologne Database for Molecular Spectroscopy CDMS. Molecules in Space. 2024; https://cdms.astro.uni-koeln.de/classic/molecules.
(41) Parker, D. S. N.; Mebel, A. M.; Kaiser, R. I. The role of isovalency in the reactions of the cyano (CN), boron monoxide (BO), silicon nitride (SiN), and ethynyl (C_2H) radicals with unsaturated hydrocarbons acetylene (C_2H_2) and ethylene (C_2H_4). *Chem. Soc. Rev.* **2014**, *43*, 2701−2713.
(42) Avery, L. W.; Broten, N. W.; MacLeod, J. M.; Oka, T.; Kroto, H. W. Detection of the heavy interstellar molecule cyanodiacetylene. *Astrophys. J.* **1976**, *205*, L173−L175.
(43) Broten, N. W.; MacLeod, J. M.; Oka, T.; Avery, L. W.; Brooks, J. W.; McGee, R. X.; Newton, L. M. Evidence for weak maser action in interstellar cyanodiacetylene. *Astrophys. J.* **1976**, *209*, L143−L147.
(44) Loomis, R. A.; Burkhardt, A. M.; Shingledecker, C. N.; Charnley, S. B.; Cordiner, M. A.; Herbst, E.; Kalenskii, S.; Lee, K. L. K.; Willis, E. R.; Xue, C.; Remijan, A. J.; McCarthy, M. C.; McGuire, B. A. An investigation of spectral line stacking techniques and application to the detection of $HC_{11}N$. *Nat. Astron.* **2021**, *5*, 188−196.
(45) Siebert, M. A.; Lee, K. L. K.; Remijan, A. J.; Burkhardt, A. M.; Loomis, R. A.; McCarthy, M. C.; McGuire, B. A. CH_3-Terminated Carbon Chains in the GOTHAM Survey of TMC-1: Evidence of Interstellar CH_3C_7N. *Astrophys. J.* **2022**, *924*, 21.
(46) Cernicharo, J.; Pardo, J. R.; Cabezas, C.; Agúndez, M.; Tercero, B.; Marcelino, N.; Fuentetaja, R.; Guélin, M.; de Vicente, P. Discovery of the C_7N^- anion in TMC-1 and IRC + 10216. *Astron. Astrophys.* **2023**, *670*, L19.
(47) Cernicharo, J.; Cabezas, C.; Pardo, J. R.; Agúndez, M.; Roncero, O.; Tercero, B.; Marcelino, N.; Guélin, M.; Endo, Y.; de Vicente, P. The magnesium paradigm in IRC + 10216: Discovery of MgC_4H^+, MgC_3N^+, MgC_6H^+, and MgC_5N^+. *Astron. Astrophys.* **2023**, *672*, L13.
(48) Cernicharo, J.; Cabezas, C.; Agúndez, M.; Endo, Y.; Tercero, B.; Marcelino, N.; de Vicente, P. QUIJOTE discovery of the cation radicals HC_5N^+ and HC_7N^+. *Astron. Astrophys.* **2024**, *686*, L15.
(49) McGuire, B. A.; Loomis, R. A.; Burkhardt, A. M.; Lee, K. L. K.; Shingledecker, C. N.; Charnley, S. B.; Cooke, I. R.; Cordiner, M. A.; Herbst, E.; Kalenskii, S.; Siebert, M. A.; Willis, E. R.; Xue, C.; Remijan, A. J.; McCarthy, M. C. Detection of two interstellar polycyclic aromatic hydrocarbons via spectral matched filtering. *Science* **2021**, *371*, 1265−1269.
(50) Kelvin Lee, K. L.; Changala, P. B.; Loomis, R. A.; Burkhardt, A. M.; Xue, C.; Cordiner, M. A.; Charnley, S. B.; McCarthy, M. C.; McGuire, B. A. Interstellar Detection of 2-cyanocyclopentadiene, C_5H_5CN, a Second Five-membered Ring toward TMC-1. *Astrophys. J. Lett.* **2021**, *910*, L2.
(51) Sita, M. L.; Changala, P. B.; Xue, C.; Burkhardt, A. M.; Shingledecker, C. N.; Kelvin Lee, K. L.; Loomis, R. A.; Momjian, E.; Siebert, M. A.; Gupta, D.; Herbst, E.; Remijan, A. J.; McCarthy, M. C.; Cooke, I. R.; McGuire, B. A. Discovery of Interstellar 2-Cyanoindene (2-C_9H_7CN) in GOTHAM Observations of TMC-1. *Astrophys. J. Lett.* **2022**, *938*, L12.
(52) Cernicharo, J.; Cabezas, C.; Fuentetaja, R.; Agúndez, M.; Tercero, B.; Janeiro, J.; Juanes, M.; Kaiser, R. I.; Endo, Y.; Steber, A. L.; Pérez, D.; Pérez, C.; Lesarri, A.; Marcelino, N.; de Vicente, P. Discovery of two cyano derivatives of acenaphthylene ($C_{12}H_8$) in TMC-1 with the QUIJOTE line survey. *Astron. Astrophys.* **2024**, *690*, L13.
(53) Kaiser, R. I.; Balucani, N. Exploring the Gas Phase Synthesis of the Elusive Class of Boronyls and the Mechanism of Boronyl Radical Reactions under Single Collision Conditions. *Acc. Chem. Res.* **2017**, *50*, 1154−1162.
(54) Frisch, M. J.; et al. *Gaussian 16*. Revision C.01; Gaussian, Inc.: Wallingford CT, 2016.
(55) Yanai, T.; Tew, D. P.; Handy, N. C. A new hybrid exchange−correlation functional using the Coulomb-attenuating method (CAM-B3LYP). *Chem. Phys. Lett.* **2004**, *393*, 51−57.
(56) Weigend, F.; Ahlrichs, R. Balanced basis sets of split valence, triple zeta valence and quadruple zeta valence quality for H to Rn: Design and assessment of accuracy. *Phys. Chem. Chem. Phys.* **2005**, *7*, 3297−3305.
(57) Grimme, S.; Antony, J.; Ehrlich, S.; Krieg, H. A consistent and accurate ab initio parametrization of density functional dispersion correction (DFT-D) for the 94 elements H-Pu. *J. Chem. Phys.* **2010**, *132*, 154104.
(58) Jacquemin, D.; Perpète, E. A.; Scalmani, G.; Frisch, M. J.; Kobayashi, R.; Adamo, C. Assessment of the efficiency of long-range corrected functionals for some properties of large compounds. *J. Chem. Phys.* **2007**, *126*, 144105.
(59) Peach, M. J. G.; Tellgren, E. I.; Sałek, P.; Helgaker, T.; Tozer, D. J. Structural and Electronic Properties of Polyacetylene and Polyyne from Hybrid and Coulomb-Attenuated Density Functionals. *J. Phys. Chem. A* **2007**, *111*, 11930−11935.
(60) Guo, X.; Zhang, J.; Zhao, Y. Ab initio characterization of size dependence of electronic spectra for linear anionic carbon clusters Cn-(n = 4−17). *J. Comput. Chem.* **2012**, *33*, 93−102.
(61) Zhang, Y.; Ning, P.; Zhang, J. Theoretical studies on structures and electronic spectra of linear free radicals CnH (n = 5−12). *Spectrochim. Acta A Mol. Biomol. Spectrosc.* **2013**, *101*, 283−293.
(62) Zhang, Y.; Li, Y.; Wang, L.; Zhang, J. Theoretical studies on the structures and electronic spectra of carbon chains CnN (n = 3−12). *Theor. Chem. Acc.* **2014**, *133*, 1420.
(63) Stasyuk, A. J.; Stasyuk, O. A.; Solà, M.; Voityuk, A. A. Cyclo[18]carbon: the smallest all-carbon electron acceptor. *Chem. Commun.* **2020**, *56*, 352−355.
(64) Grimme, S. Semiempirical hybrid density functional with perturbative second-order correlation. *J. Chem. Phys.* **2006**, *124*, 034108.
(65) Curtiss, L. A.; Redfern, P. C.; Raghavachari, K. Gaussian-4 theory. *J. Chem. Phys.* **2007**, *126*, 084108.
(66) Suntsova, M. A.; Dorofeeva, O. V. Use of G4 Theory for the Assessment of Inaccuracies in Experimental Enthalpies of Formation of Aromatic Nitro Compounds. *J. Chem. Eng. Data* **2016**, *61*, 313−329.
(67) Dorofeeva, O. V.; Ryzhova, O. N. Accurate estimation of enthalpies of formation for C-, H-, O-, and N-containing compounds using DLPNO-CCSD(T1)/CBS method. *Struct. Chem.* **2021**, *32*, 553−563.
(68) Bâldea, I. Long Carbon-Based Chains of Interstellar Medium Can Have a Triplet Ground State. Why Is This Important for Astrochemistry? *ACS Earth Space Chem.* **2019**, *3*, 863−872.
(69) Etim, E. E.; Gorai, P.; Das, A.; Chakrabarti, S. K.; Arunan, E. Systematic theoretical study on the interstellar carbon chain molecules. *Astrophys. J.* **2016**, *832*, 144.
(70) Knizia, G. Intrinsic Atomic Orbitals: An Unbiased Bridge between Quantum Theory and Chemical Concepts. *J. Chem. Theory Comput.* **2013**, *9*, 4834−4843.
(71) Ochterski, J. W. *Thermochemistry in Gaussian*; Gaussian Inc: Pittsburgh PA, 2000; pp 1−19.

(72) Curtiss, L. A.; Raghavachari, K.; Redfern, P. C.; Pople, J. A. Assessment of Gaussian-2 and density functional theories for the computation of enthalpies of formation. *J. Chem. Phys.* **1997**, *106*, 1063−1079.
(73) Yañez, O.; Báez-Grez, R.; Inostroza, D.; Rabanal-León, W. A.; Pino-Rios, R.; Garza, J.; Tiznado, W. AUTOMATON: A Program That Combines a Probabilistic Cellular Automata and a Genetic Algorithm for Global Minimum Search of Clusters and Molecules. *J. Chem. Theory Comput.* **2019**, *15*, 1463−1475.
(74) Yañez, O.; Inostroza, D.; Usuga-Acevedo, B.; Vásquez-Espinal, A.; Pino-Rios, R.; Tabilo-Sepulveda, M.; Garza, J.; Barroso, J.; Merino, G.; Tiznado, W. Evaluation of restricted probabilistic cellular automata on the exploration of the potential energy surface of Be6B11-. *Theor. Chem. Acc.* **2020**, *139*, 41.
(75) Perdew, J. P.; Burke, K.; Ernzerhof, M. Generalized Gradient Approximation Made Simple. *Phys. Rev. Lett.* **1996**, *77*, 3865−3868.
(76) Glendening, E. D.; Badenhoop, J. K.; Reed, A. E.; Carpenter, J. E.; Bohmann, J. A.; Morales, C. M.; Karafiloglou, P.; Landis, C. R.; Weinhold, F. *NBO 7.0*; Theoretical Chemistry Institute, University of Wisconsin: Madison. 2018.
(77) Glendening, E. D.; Landis, C. R.; Weinhold, F. NBO 7.0: New vistas in localized and delocalized chemical bonding theory. *J. Comput. Chem.* **2019**, *40*, 2234−2241.
(78) Zhai, H. J.; Chen, Q.; Bai, H.; Li, S. D.; Wang, L. S. Boronyl chemistry: The BO group as a new ligand in gas-phase clusters and synthetic compounds. *Acc. Chem. Res.* **2014**, *47*, 2435−2445.
(79) Maity, S.; Dangi, B. B.; Parker, D. S. N.; Kaiser, R. I.; Lin, H.-M.; E, H.-P.; Sun, B.-J.; Chang, A. H. H. Combined Crossed Molecular Beam and Ab Initio Investigation of the Reaction of Boron Monoxide (BO; $X^2\Sigma^+$) with 1,3-Butadiene ($CH_2CHCHCH_2$; X^1Ag) and Its Deuterated Counterparts. *J. Phys. Chem. A* **2015**, *119*, 1094−1107.
(80) Taniguchi, K.; Gorai, P.; Tan, J. C. Carbon-chain chemistry in the interstellar medium. *Astrophys. Space Sci.* **2024**, *369*, 34.
(81) Puzzarini, C.; Stanton, J. F.; Gauss, J. Quantum-chemical calculation of spectroscopic parameters for rotational spectroscopy. *Int. Rev. Phys. Chem.* **2010**, *29*, 273−367.
(82) Santos, J. C.; Rocha, A. B.; Oliveira, R. R. Rotational spectrum simulations of asymmetric tops in an astrochemical context. *J. Mol. Model.* **2020**, *26*, 278.
(83) Alessandrini, S.; Melosso, M.; Rivilla, V. M.; Bizzocchi, L.; Puzzarini, C. Computational Protocol for the Identification of Candidates for Radioastronomical Detection and Its Application to the C_3H_3NO Family of Isomers. *Molecules* **2023**, *28*, 3226.
(84) Tanimoto, M.; Saito, S.; Hirota, E. Microwave spectrum of the boron monoxide radical BO. *J. Chem. Phys.* **1986**, *84*, 1210−1214.
(85) Melen, F.; Dubois, I.; Bredohl, H. The A-X and B-X transitions of BO. *J. Phys. B: At. Mol. Opt. Phys.* **1985**, *18*, 2423−2432.
(86) Mehringer, D. M.; Snyder, L. E.; Miao, Y.; Lovas, F. J. Detection and Confirmation of Interstellar Acetic Acid. *Astrophys. J.* **1997**, *480*, L71−L74.
(87) Brown, R. D.; Crofts, J. G.; Godfrey, P. D.; Gardner, F. F.; Robinson, B. J.; Whiteoak, J. B. Discovery of interstellar methyl formate. *Astrophys. J.* **1975**, *197*, L29.
(88) Churchwell, E.; Winnewisser, G. Observations of methyl formate in the galactic center. *Astron. Astrophys.* **1975**, *45*, 229−231.
(89) Hollis, J. M.; Lovas, F. J.; Jewell, P. R. Interstellar Glycolaldehyde: The First Sugar. *Astrophys. J.* **2000**, *540*, L107−L110.
(90) Rivilla, V. M.; et al. Precursors of the RNA World in Space: Detection of (Z)-1,2-ethenediol in the Interstellar Medium, a Key Intermediate in Sugar Formation. *Astrophys. J. Lett.* **2022**, *929*, L11.
(91) Lattelais, M.; Pauzat, F.; Ellinger, Y.; Ceccarelli, C. Interstellar Complex Organic Molecules and the Minimum Energy Principle. *Astrophys. J.* **2009**, *696*, L133−L136.
(92) Laas, J. C.; Garrod, R. T.; Herbst, E.; Widicus Weaver, S. L. Contributions from Grain Surface and Gas Phase Chemistry to the Formation of Methyl Formate and its Structural Isomers. *Astrophys. J.* **2011**, *728*, 71.
(93) Quitián-Lara, H. M.; Fantuzzi, F.; Mason, N. J.; Boechat-Roberty, H. M. Decoding the molecular complexity of the solar-type protostar NGC 1333 IRAS 4A. *Mon. Not. R. Astron. Soc.* **2023**, *527*, 10294−10308.
(94) Loomis, R. A.; McGuire, B. A.; Shingledecker, C.; Johnson, C. H.; Blair, S.; Robertson, A.; Remijan, A. J. Investigating the Minimum Energy Principle in Searches for New Molecular Species—The Case of H_2C_3O Isomers. *Astrophys. J.* **2015**, *799*, 34.
(95) Lattelais, M.; et al. Differential adsorption of complex organic molecules isomers at interstellar ice surfaces. *Astron. Astrophys.* **2011**, *532*, A12.
(96) Fantuzzi, F.; Baptista, L.; Rocha, A. B.; Boechat-Roberty, H. M. Positive molecular ions and ion-neutral complexes in the gas phase: Structure and stability of $C_2H_4O_2^{+\cdot}$ and $C_2H_4O_2^{2+}$ isomers. *Int. J. Quantum Chem.* **2012**, *112*, 3303−3311.
(97) Londoño-Restrepo, J.; Gómez, S.; Quitián-Lara, H. M.; Fantuzzi, F.; Restrepo, A. More π, please: What drives the formation of unsaturated molecules in the interstellar medium? *Chem. Sci.* **2025**, *16*, 3051−3065.
(98) Quitián-Lara, H. M.; Fantuzzi, F.; Oliveira, R. R.; Nascimento, M. A. C.; Wolff, W.; Boechat-Roberty, H. M. Dissociative single and double photoionization of biphenyl ($C_{12}H_{10}$) by soft X-rays in planetary nebulae. *Mon. Not. R. Astron. Soc.* **2020**, *499*, 6066−6083.
(99) Santos, J. C.; Fantuzzi, F.; Quitián-Lara, H. M.; Martins-Franco, Y.; Menéndez-Delmestre, K.; Boechat-Roberty, H. M.; Oliveira, R. R. Multiply charged naphthalene and its $C_{10}H_8$ isomers: bonding, spectroscopy, and implications in AGN environments. *Mon. Not. R. Astron. Soc.* **2022**, *512*, 4669−4682.
(100) Panda, S.; Sivadasan, D.; Job, N.; Sinjari, A.; Thirumoorthy, K.; Anoop, A.; Thimmakondu, V. S. Why Are MgC_3H Isomers Missing in the Interstellar Medium? *J. Phys. Chem. A* **2022**, *126*, 4465−4475.
(101) Gomes, A. K. M. S.; Oliveira, R. R.; Cardozo, T. M.; Fantuzzi, F. Linear or Cyclic? Theoretical Investigation of Astrophysically Relevant Magnesium-Bearing MgC_nH Carbon Chains and Related Isomers. *J. Comput. Chem.* **2025**, *46*, No. e70031.
(102) Parker, D. S. N.; Zhang, F.; Maksyutenko, P.; Kaiser, R. I.; Chang, A. H. H. A crossed beam and ab initio investigation of the reaction of boron monoxide (^{11}BO; $X^2\Sigma^+$) with acetylene (C_2H_2; $X^1\Sigma_g^+$). *Phys. Chem. Chem. Phys.* **2011**, *13*, 8560−8570.
(103) Parker, D. S. N.; Balucani, N.; Stranges, D.; Kaiser, R. I.; Mebel, A. A Crossed Beam and ab Initio Investigation on the Formation of Boronyldiacetylene ($HCCCC^{11}BO$; $X^1\Sigma^+$) via the Reaction of the Boron Monoxide Radical (^{11}BO; $X^2\Sigma^+$) with Diacetylene (C_4H_2; $X^1\Sigma_g^+$). *J. Phys. Chem. A* **2013**, *117*, 8189−8198.
(104) Millar, T. J.; Walsh, C.; Field, T. A. Negative Ions in Space. *Chem. Rev.* **2017**, *117*, 1765−1795.
(105) Martinez, O.; Yang, Z.; Demarais, N. J.; Snow, T. P.; Bierbaum, V. M. Gas-Phase Reactions of Hydride Anion, H^-. *Astrophys. J.* **2010**, *720*, 173−177.

https://doi.org/10.1021/acsearthspacechem.5c00089
ACS Earth Space Chem. 2025, 9, 2045−2055